

THE NEW VARSKIN 4 PHOTON SKIN DOSIMETRY MODEL

D. M. Hamby¹, C. J. Lodwick¹, T. S. Palmer¹, S. R. Reese¹, K. A. Higley¹, J. A. Caffrey^{1,*}, S. Sherbini², M. Saba² and S. P. Bush-Goddard²

¹Department of Nuclear Engineering and Radiation Health Physics, Oregon State University, Corvallis, OR 97331-5902, USA

²Nuclear Regulatory Commission, Office of Nuclear Regulatory Research, Rockville, MD 20852, USA

*Corresponding author: caffreyj@onid.orst.edu

Received December 16 2011, revised August 28 2012, accepted September 3 2012

A new photon skin dosimetry model, described here, was developed as the basis for the enhanced VARSKIN 4 thin tissue dosimetry code. The model employs a point-kernel method that accounts for charged particle build-up, photon attenuation and off-axis scatter. Early comparisons of the new model against Monte Carlo particle transport simulations show that VARSKIN 4 is highly accurate for very small sources on the skin surface, although accuracy at shallow depths is compromised for radiation sources that are on clothing or otherwise elevated from the skin surface. Comparison results are provided for a one-dimensional point source, a two-dimensional disc source and three-dimensional sphere, cylinder and slab sources. For very small source dimensions and sources in contact with the skin, comparisons reveal that the model is highly predictive. With larger source dimensions, air gaps or the addition of clothing between the source and skin; however, VARSKIN 4 yields over-predictions of dose by as much as a factor of 2 to 3. These cursory Monte Carlo comparisons confirm that significant accuracy improvements beyond the previous version were achieved for all geometries. Improvements were obtained while retaining the VARSKIN characteristic user convenience and rapid performance.

INTRODUCTION

An improved photon skin dosimetry model was developed and implemented within the VARSKIN 4⁽¹⁾ deterministic thin tissue dosimetry code. The improvement was largely motivated by the need to address the previous code's over-predictions at shallow skin depths, but also to extend the model's application with larger source geometries and to eliminate some over-simplifications. The new model employs a point-kernel method that considers the buildup of charged particles, transient-charged particle equilibrium (CPE), photon attenuation and off-axis scatter. Many of the basic input restrictions applied in previous versions of VARSKIN are carried into the improved model, namely that the source can be a point, disc, cylinder, sphere or slab; and that dose is calculated to an averaging disc beneath the skin surface at any depth, and for dose averaging areas of between 0.01 and 100 cm². Comparisons of VARSKIN 4 with the MCNP5 Monte Carlo particle transport code⁽²⁾ reveal that the new photon dosimetry model is accurate for very small or very thin sources on the skin surface. Agreement weakens for large volume sources or for sources that are lifted away from the skin surface, such as a source adhered to clothing. A comprehensive overview of the relevant concepts and assumptions can be found in the NUREG/CR-6918, Rev. 1⁽¹⁾ that accompanies VARSKIN 4, as provided by

the Radiation Safety Information Computational Center (<http://rsicc.ornl.gov/>).

The previous version, VARSKIN 3⁽³⁾, significantly overestimated photon skin dose at shallow depths of less than a few hundred microns, primarily due to its inadequate accounting for charged particle buildup. The photon model used a library of gamma-ray exposure constants to estimate dose at the desired depth in tissue. It attempted to correct for the absence of CPE as a function of the average photon energy, but inadequately addressed contributions from higher-energy photons. Comparisons with Monte Carlo simulations at various photon energies and skin depths revealed that VARSKIN 3 overestimated dose with increasing photon energy, up to a factor of 5 at 1.5 MeV.

Photon doses typically contribute only a small fraction of the total skin dose in cases of skin contamination, particularly for cases of direct contact with no protective layer. Many contaminant radionuclides however emit beta radiation of relatively low-energy accompanied by relatively high-energy gamma photons. Such scenarios may result in dominating contributions of shallow skin dose from photons: an effect that is further magnified with protective material between the contamination and the skin. The Nuclear Regulatory Commission therefore sought to develop a more refined photon dose algorithm to correct the various deficiencies of the prior VARSKIN model.

THE VARSKIN 4 PHOTON DOSIMETRY MODEL

An explanation of the dose model begins with the simple instance of a volume of tissue exposed to a uniform fluence of uncollided photons, Φ_0 , of energy, E , from a point source in a homogeneous medium. Ignoring attenuation and assuming that CPE is established, the dose to any and every point in that volume of tissue is

$$D(E) = \Phi_0 \cdot E \cdot \left(\frac{\mu_{\text{en}}(E)}{\rho} \right)_{\text{tissue}} \quad (1)$$

where $(\mu_{\text{en}}(E)/\rho)_{\text{tissue}}$ is the energy-dependent mass energy absorption coefficient for tissue^(4, 5). The assumption is made for this calculation that the dose volume is infinitely thin and that interactions occur in two-dimensions normal to a beam of incident photons. The uncollided fluence originating from a point source is therefore determined by

$$\Phi_0 = \frac{S}{4\pi d^2} \quad (2)$$

where S has units of photons emitted per nuclear transition (i.e. yield), and d is the kernel distance between the source and dose locations, in an infinitely large homogeneous volume. Thus, a point-kernel tissue dose per transition at distance, d , from a point source can be calculated for radionuclides emitting i photons of energy E_i and yield y_i , given that

$$\begin{aligned} \text{Dose} \left[\frac{\text{Gy}}{\text{nt}} \right] &= \frac{k(\text{J g/MeV kg})}{4\pi d^2(\text{cm}^2)} \\ &\times \sum_{i=1}^N \left[y_i \left[\frac{\text{photon}}{\text{nt}} \right] \cdot E_i \left(\frac{\text{MeV}}{\text{photon}} \right) \right. \\ &\times \left. \left(\frac{\mu_{\text{en}}(E_i)}{\rho} \right)_{\text{tis}} \left(\frac{\text{cm}^2}{\text{g}} \right) \right] \end{aligned} \quad (3)$$

where N is the number of photons specified for the nuclide and $k = 1.602 \times 10^{-10} (\text{J g/MeV kg})$.

If the point source is assumed to rest on the air/skin interface, and a profile of dose with depth in tissue is of interest, Equation (3) must be modified to account for the attenuation of photons in tissue, charged particle buildup and electron scatter at shallow depths leading to CPE. To account for attenuation as photons travel through tissue, the uncollided photon fluence is decreased by the factor, $e^{-\mu d}$, where μ is the energy-dependent linear attenuation coefficient for tissue (VARSKIN 4 coefficients are taken from ICRU 44)⁽⁶⁾.

For CPE, Attix⁽⁴⁾ states that the condition exists if, in an infinitely small volume, ‘... each charged

particle of a given type and energy leaving [the volume] is replaced by an identical particle of the same energy entering, in terms of expectation values.’ In order for dose at shallow depths to be calculated accurately, the CPE as a function of depth must be determined. The VARSKIN 4 determination of CPE is based on Monte Carlo (MCNP5) simulations as the difference between energy released (KERMA; F6 tally) and energy absorbed (dose; *F8 tally).

Because the energy transfer from photons and energy absorption from the resulting charged particles do not occur in the same location⁽⁷⁾, there is a ‘buildup region’ in which dose is zero at the skin surface and then increases until a depth is reached at which dose and KERMA are equal. The depth at which equilibrium occurs is approximately equal to the range of the most energetic electron created by the incident photons⁽⁷⁾. The energy-dependent factor accounting for CPE buildup (f_{cpe}) is the ratio of dose, D , to KERMA, K , for a particular incident photon energy at a given tissue depth, such that,

$$f_{\text{cpe}}(E, d) = \frac{D(E, d)}{K(E, d)} \quad (4)$$

In considering CPE along with attenuation, a proportional relationship between dose and KERMA develops as a function of depth within a medium⁽⁴⁾; this relationship is referred to as ‘transient CPE’. Dose reaches a maximum ‘... at the depth where the rising slope due to buildup of charged particles is balanced by the descending slope due to attenuation’⁽⁴⁾, after which dose decreases with depth because of the dominating effect of photon attenuation. At the point where transient CPE occurs, dose is essentially equal to KERMA for low-energy photons and the value of f_{cpe} is unity (1). As photon energy increases beyond ~ 1 MeV, this assumption of dose and KERMA equality begins to fail due to the increasing fraction of bremsstrahlung, but not to the extent that it appreciably affects deep dose estimations. Based upon comparisons with Monte Carlo simulations of shallow and deep tissue dose, the VARSKIN 4 model limits the value of f_{cpe} to 1.05, thereby allowing dose to exceed KERMA by a maximum of 5 % at depth. This limitation is important only for higher energy photons.

The empirical function for f_{cpe} used in VARSKIN 4 is,

$$f_{\text{cpe}}(x) = \left(a + b \cdot \ln(x) + \frac{c}{\sqrt{x}} \right)^{-1} \quad (5)$$

where x (cm) is equal to the point-kernel distance between source point and dose point, and the

coefficients a , b and c are functions of initial photon energy (in keV) as described in Equations (6)–(8),

$$a = 19.78 + 0.1492 E \cdot \ln(E) - 0.008390 E^{1.5} + 0.00003624 E^2 + 3.343 \sqrt{E} \cdot \ln(x) - \frac{10.72 E}{\ln(E)} \quad (6)$$

$$b = 1.217 \times 10^{-12} E^4 - 5.673 \times 10^{-9} E^3 + 7.942 \times 10^{-6} E^2 - 0.002028 E + 0.3296 \quad (7)$$

$$c = 9.694 \times 10^{-13} E^4 - 4.861 \times 10^{-9} E^3 + 7.765 \times 10^{-6} E^2 - 0.001856 E + 0.1467 \quad (8)$$

Estimates of f_{cpe} were determined for dose kernels with trajectories normal to the skin surface. At any given distance from the skin surface, however, the fractional CPE for full point-kernel calculations may vary considerably. Dose kernels with angled trajectories directed nearer the averaging disc boundary result in an added probability of escape for energetic particles near the air-tissue interface. Such energy losses are more prominent for energetic photons as both the probability of Compton interaction and the range of secondary electrons increase, generally beginning at photon energies of greater than a few hundred kiloelectron volt. This scatter of energy out of tissue is included in the model by considering an off-axis scatter factor, F_{oa} . The factor, taking on values between zero and one, is necessary only for point-kernel calculations in which the angle between the central axis at the surface and the dose point is $>70^\circ$ from normal, and for photon energies of >300 keV. For all other cases F_{oa} is set to unity (1). The off-axis scatter factor is calculated from data obtained through Monte Carlo simulation and is represented in VARSKIN 4 by the empirical function,

$$F_{\text{oa}} = (-1.57 + 0.000334 \theta^{2.5} - 0.0000325 \theta^3) (0.93 + 0.1R) \quad (9)$$

where R is the radius of the dose-averaging disc and θ is the off-axis scatter angle (in degrees).

Fully accounting for charged particle buildup, attenuation and scatter, Equation (3) now becomes

$$\text{Dose} \left[\frac{\text{Gy}}{\text{nt}} \right] = \frac{k}{4\pi d^2} \cdot \sum_{i=1}^N \times \left[y_i \cdot E_i \cdot \left(\frac{\mu_{\text{en}}(E_i)}{\rho} \right)_{\text{tissue}} \times (f_{\text{cpe}})_i \cdot (F_{\text{oa}})_i \cdot e^{-\mu(E_i) \cdot d} \right] \quad (10)$$

Title 10, Section 20.1201(c), of the Code of Federal Regulations requires, ‘the assigned shallow-dose equivalent (at a depth of 7 mg cm^{-2}) must be the dose averaged over the contiguous 10 cm^2 of skin receiving the highest exposure.’ In order to determine average dose at depth from a source at the surface, an integration of Equation (10) over the averaging area must be executed. No closed-form solution can be determined, however, when integrating the exponential term. A step-wise numerical integration of Equation (10) is instead performed, in essence providing the averaged dose for every point kernel pair of locations between the source volume and the infinitely thin dose averaging disc.

Studies were conducted in support of the numerical integration method to determine a method of segmentation that produced consistently accurate results using the fewest required number of segments. As detailed in the NUREG⁽¹⁾, three methods were investigated: (1) segments determined by equal radii of the dose-averaging disc; (2) segments determined by equal off-axis angles and (3) segments determined by equal annular area. Results indicated that segments divided according to equal lengths (radii) along the radius of the averaging disc converged upon consistently accurate solutions using the least segmentation, with divisions by equal annular area requiring the largest number of segments. Highly consistent solutions were achieved when calculated with no fewer than 300 segmentations for equal lengths along the radius of a 10 cm^2 averaging disc. The VARSKIN 4 numerical integration therefore utilises 300 segments along the radius of the dose region, although fewer segments were required for equivalent precision when analysing a smaller averaging disc (Figure 1).

The dose per nuclear transition for a given point source radionuclide with N emissions, averaged over an infinitely thin disc of radius R , at normal depth in tissue h is therefore calculated by

$$D(h, R) \left[\frac{\text{Gy}}{\text{nt}} \right] = \frac{k}{4\pi} \cdot \sum_{j=1}^L \left[\frac{w_j}{d_j^2} \cdot \sum_{i=1}^N \left[y_i \cdot E_i \times \left(\frac{\mu_{\text{en}}(E_i)}{\rho} \right)_{\text{tis}} \cdot (f_{\text{cpe}})_{ij} \cdot (F_{\text{oa}})_{ij} \cdot e^{-\mu(E_i) \cdot d_j} \right] \right] \quad (11)$$

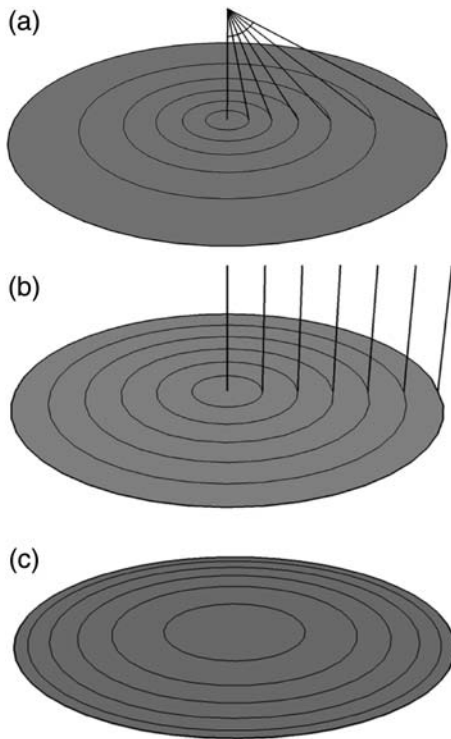


Figure 1. Graphic depictions for each of the studied dose segmentation techniques: (a) Equal projection angle increments; (b) Equal radial increments and (c) Equal annular area. VARSKIN 4 utilises equal radial increments in its numerical integrations.

where $d_j = \sqrt{(h^2 + r_j^2)}$, with r_j and w_j representing the annular radius and fractional area weight, respectively, for each of the L dose region segments in the numerical integration.

To this point, the model describes photon treatment for cases in which the source is an isotropic point located directly above and on axis with the centre of the dose region, assuming radial symmetry of the dose-averaging disc (Figure 2a). In order to extend the model to handle point-kernel calculations for volumetric sources or multiple point sources, considerations must be taken for cases in which the point source is off-axis from centre and either still within or completely removed from the averaging disc projection. The implication is simply a geometric determination of the distance between each source and dose point kernel, including an area-weighted factor for each radially symmetric dose location on the averaging disc.

In the first case, where the point source is off-axis yet still over the averaging disc, there is symmetry along a diameter of the dose-averaging disc. The

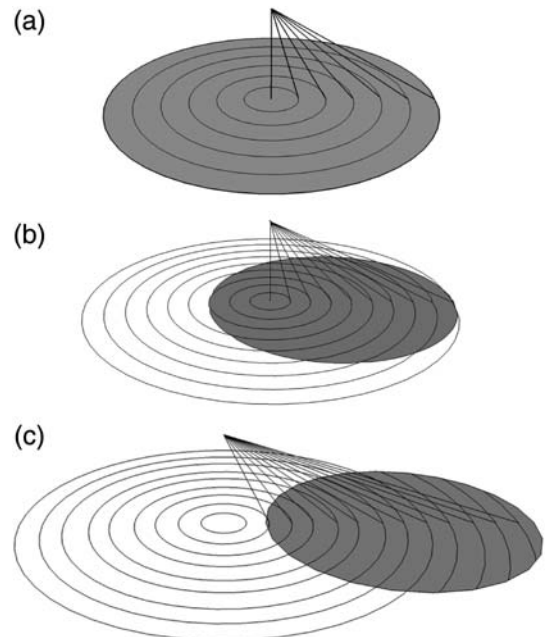


Figure 2. Point source depictions: (a) Point source on axis above tissue averaging disc; (b) Point source above averaging disc but off axis and (c) Point source off axis and not directly above averaging disc.

average of the point-kernel doses is determined by a weighting of doses calculated along the diameter. The calculation begins by projecting the dose point to the averaging disc, normal to the skin surface. The averaging disc then is divided into a series of concentric annuli about the projected dose point, until the radius of the annuli reaches the nearest edge of the averaging disc. Thereafter, the weighting model transitions to a series of arcs passing through the averaging disc (Figure 2b). In the case where the point source is removed from the projected dose region entirely, the weighting model uses only concentric arcs (Figure 2c). In either off-axis scenario, the annuli and arcs are representative of regions with equal dose. Point-kernel dose is calculated along the diameter in each of the 300 segments defined by the differential annuli and arcs and then weighted by the fractional area of each segment. Volume averaging may also be implemented, wherein the dose calculation to the averaging disc is repeated and averaged at ten evenly distributed depths within a user-defined dose volume.

In the case of volume and area sources, the application of symmetry used to efficiently calculate dose requires that the source centreline remains on axis with the dose averaging disc. For slab source geometries, source kernels are created in equal symmetric increments at 15 locations in each of the three

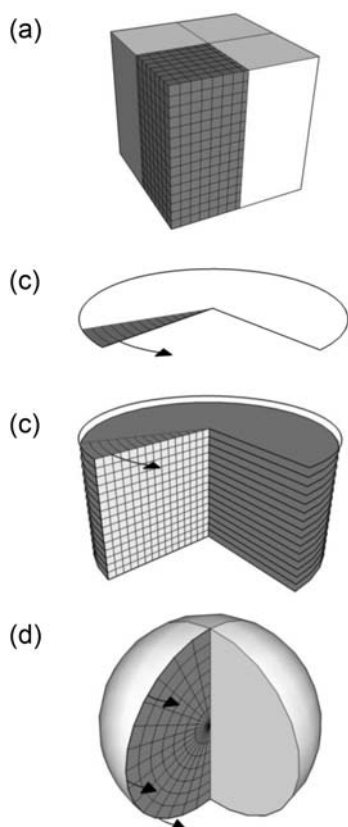


Figure 3. Depictions of (a) slab, (b) disc, (c) cylindrical and (d) spherical distributed sources. Total dose calculated as the sum of point kernels weighted by volume/area for each source region. Arrows indicate radial symmetry about the dose region central axis.

dimensions within the source volume, such that 15^3 source kernels are represented. Dose is then calculated from a point source centred within each region, though in practice the application of symmetry requires calculations from only one quadrant of the slab. Final dose is then determined as four times the sum of each kernel dose weighted by the region volume to account for the partial volumes created by planes of symmetry (Figure 3a). For disc sources, dose kernels are calculated for each of 15 equally spaced concentric annuli. Radial symmetry permits treatment of each kernel as a point source weighted according to the annular area (Figure 3b). Cylindrical sources are effectively treated as a series of 15 evenly distributed disc sources, where each of the 15^2 annular kernels is weighted according to the corresponding volume (Figure 3c). Spherical sources use 15^2 annular kernels as well, but axial distribution is here determined instead by 15 equal divisions of the inclination angle (Figure 3d).

The new VARSKIN 4 photon dosimetry model takes into consideration attenuation in cover materials and air between source and skin. As with the beta dosimetry model, up to five layers above the skin are allowed, including an optional air gap only above the skin surface. Other material layers are restricted to cotton and/or latex, as they remain highly representative of the most likely materials to be contaminated and modelled in practice. Source materials in the photon model are not required and are assumed to have the same characteristics as air. Based on calculations of the attenuation factor, effects of attenuation above the skin surface are insignificant for very small volumetric sources and for photon energies above ~ 50 keV. Additionally, the f_{cpe} factor is assumed to be the same for all materials based on an assumption that any buildup in air or thin covers would be insignificant in comparison to that in tissue.

DISCUSSION

The photon dosimetry model of VARSKIN 4 shows considerable improvement over the previous version. The data indicate that, for volumetric sources with a maximum linear dimension less than ~ 100 μm , the assumption that the source material is similar to air is of no consequence for photon energies between 10 keV and 3 MeV. As the source dimensions increase in size, VARSKIN 4 overestimates dose for photon energies less than ~ 40 keV due to the underestimation of self-shielding. Results also indicate that air and tissue are quite similar in terms of attenuation over very short distances (i.e. < 5 mm).

VARSKIN 4 results are provided for a one-dimensional point source, a two-dimensional disc source and three-dimensional sphere, cylinder and slab sources. Figure 4 presents dose rate to tissue from various point sources as a function of tissue depth.

The simplest calculation in VARSKIN 4 is the scenario in which a point source is located directly on the skin surface and on the axis with the dose-averaging area. When compared with MCNP5, the VARSKIN 4 model performs very well for low- and high-energy photons at all depths (Figure 4). A notable point of Figure 4 is that the photon dose at shallow depths for ^{60}Co and $^{137\text{m}}\text{Ba}$ first increases and then decreases, showing a dose buildup region for which the previous version did not account. The VARSKIN 4 model also effectively accounts for attenuation of photons through the skin (Figure 4b). VARSKIN 4 over-predicts dose by of ~ 10 % for tissue depths of highest dose between ~ 0.030 and 0.130 cm for the photons of ^{60}Co (Figure 4). However, the depth-dose curves for $^{99\text{m}}\text{Tc}$ and ^{238}U reach their maximum almost immediately (at least by 50 μm), due to their abundant yield of low-energy photons. Dose estimates are also provided

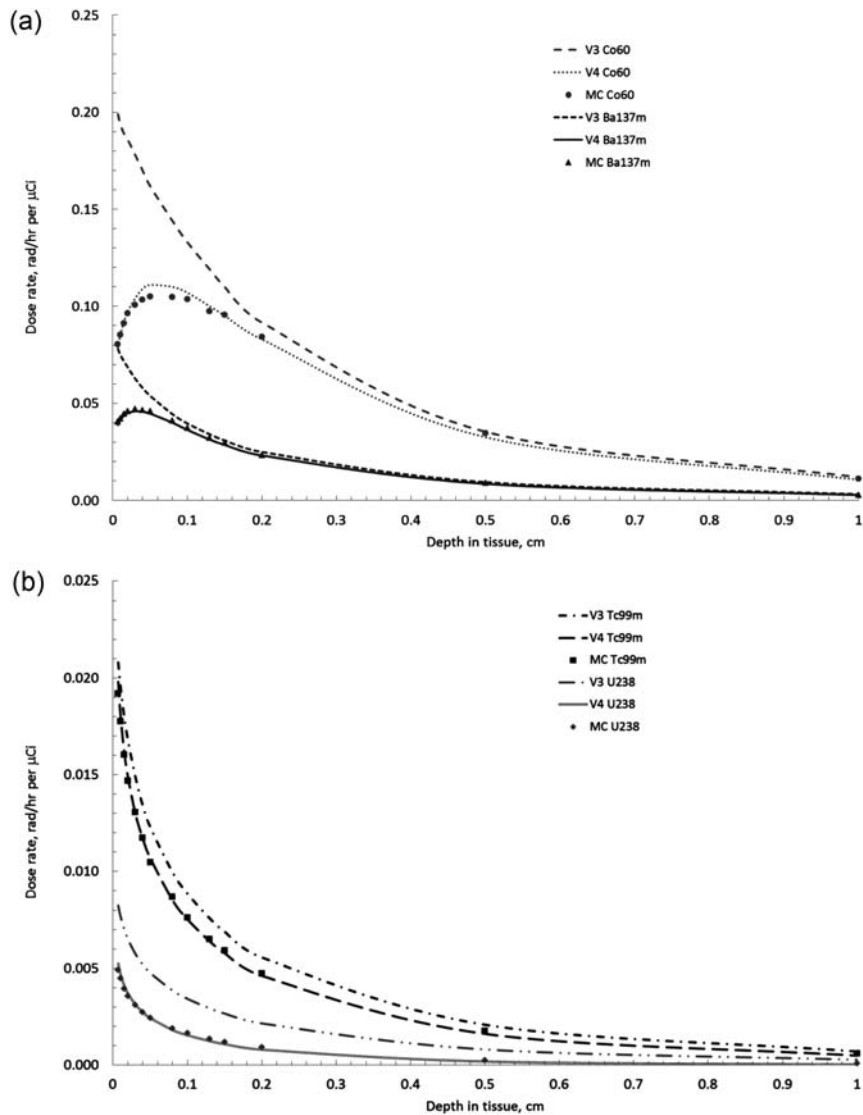


Figure 4. Photon dose rate for a 1 cm^2 dose averaging area as a function of depth for (a) ^{60}Co and $^{137\text{m}}\text{Ba}$, and (b) $^{99\text{m}}\text{Tc}$ and ^{238}U . In all cases the source is modelled as a point resting directly on the surface of the skin. MCNP5 standard error was $<5\%$ in all cases.

from VARSKIN 3 to illustrate the improvements developed by VARSKIN 4 at shallow depths.

The four panels of Figure 5 show relative dose as a function of photon energy and dose averaging area at the shallow depth of 7 mg cm^{-2} in tissue for calculations of disc, sphere, cylinder and slab sources. The panels in Figure 6 show the same dose calculations, but at the depth of 300 mg cm^{-2} . Plots similar to Figure 6 for deeper penetration depths show that the VARSKIN 4 model is extremely reliable at depths $>300\text{ mg cm}^{-2}$. As shown in Figures 5 and

6, the VARSKIN 4 model performs well in the 2D disc source geometry, again because the source point in each kernel calculation rests on the skin surface. When the source kernel moves above the skin surface, as in the volumetric source geometry, the deviation between VARSKIN 4 and MCNP5 increases due to its handling of the gap created between source and skin in the point-kernel calculation. At a depth of 7 mg cm^{-2} (Figure 5), the skin dose from volumetric geometries is over-predicted by VARSKIN 4 for photon energies greater than ~ 600

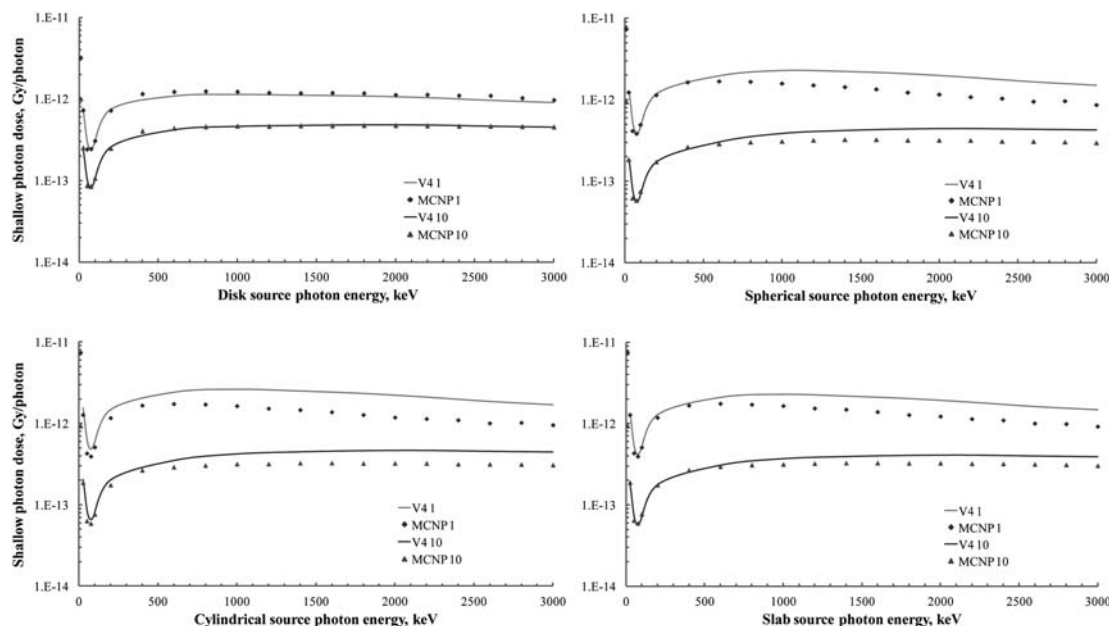


Figure 5. Comparison of shallow (7 mg cm^{-2}) tissue dose for four geometry scenarios (2D disc and 3D sphere, cylinder and cube) with 1 mm dimensions for 1 cm^2 (lighter line) and 10 cm^2 (darker line) dose-averaging areas. Lines represent VARSKIN 4 results and points represent MCNP5 results for a (a) disc source; (b) spherical source; (c) cylindrical source and (d) slab source. MCNP5 standard error was $< 5\%$ in all cases.

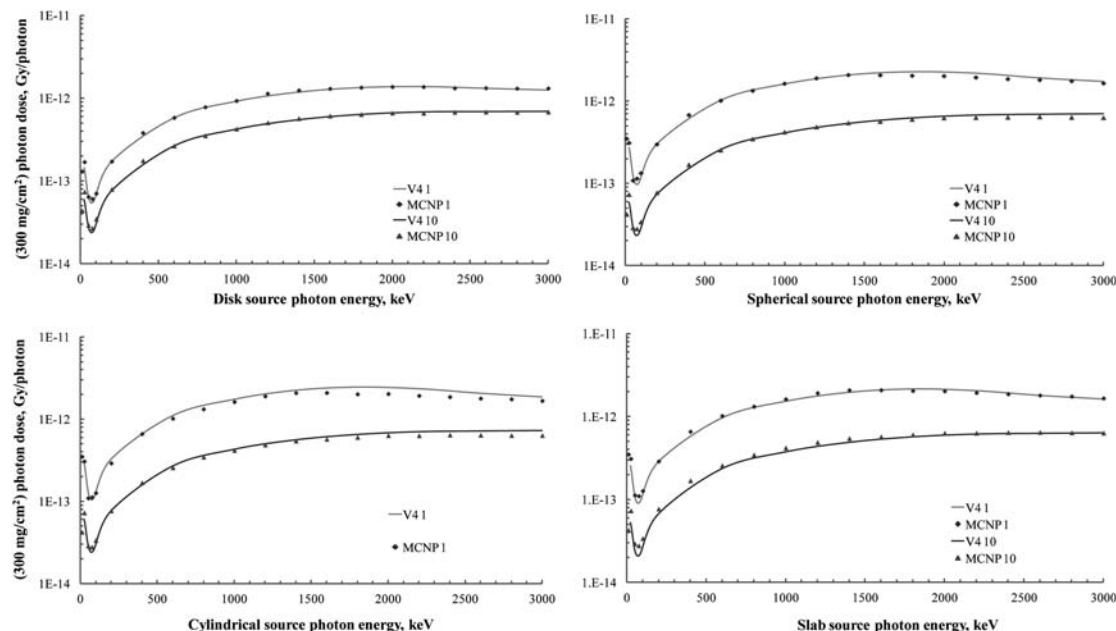


Figure 6. Comparison of tissue dose at 300 mg cm^{-2} for four geometry scenarios (2D disc and 3D sphere, cylinder and cube) with 1 mm dimensions for 1 cm^2 (lighter line) and 10 cm^2 (darker line) dose-averaging areas. Lines represent VARSKIN 4 results and points represent MCNP5 results for a (a) disc source; (b) spherical source; (c) cylindrical source and (d) slab source. MCNP5 standard error was $< 5\%$ in all cases.

keV. This over-prediction is most likely the result of a physical disruption of charged particle buildup throughout the source and at the source/tissue interface, a phenomenon not considered within the VARSKIN model. These discrepancies are not evident at a depth of 300 mg cm^{-2} (Figure 6) for the various source geometries, as CPE at that depth is well established. Studies continue in order to examine changes in CPE in the skin when the kernel source is removed from direct contact with the surface by air or clothing.

The addition of protective clothing in the photon dosimetry model serves to add simple material attenuation through each layer of media, as the point-kernel method inherently accounts for geometric attenuation caused by separation between the source and tissue. This separation results in the physical disruption of charged particle buildup; VARSKIN 4 handles this disruption only in the sense that buildup is assumed not to begin until the photons reach the skin surface. Additional comparisons for these can be found in the NUREG⁽¹⁾.

CONCLUSIONS

The new VARSKIN photon dosimetry model now incorporates material attenuation and charged particle buildup, providing significant improvements to the calculation of photon dose at shallow depths in tissue. For very small source dimensions and sources in contact with the skin, comparisons with MCNP5 show that the model is highly predictive. With larger source dimensions, air gaps or the addition of clothing between the source and skin, however, VARSKIN 4 calculations produce over-predictions by as much as a factor of 2 to 3. These considerable improvements to the VARSKIN photon dosimetry

model are incorporated with little additional computational expense as a result of the efficient treatment for the deterministic numerical integration of the point kernel dose methodology.

FUNDING

This work was supported by the United States Nuclear Regulatory Commission (RES-08-137). Any opinions or positions expressed in this paper are solely those of the authors and do not reflect official agency positions.

REFERENCES

1. Hamby, D. M., Lodwick, C. J., Palmer, T. S., Reese, S. R. and Higley, K. A. *VARSKIN 4: A computer code for skin contamination dosimetry*. USNRC Report NUREG/CR-6918, Rev 1. U.S. Nuclear Regulatory Commission. (2011).
2. X-5 Monte Carlo Team. *MCNP—A general Monte Carlo N-particle transport code, Version 5*. LANL Report LA-CP-03-0245. Los Alamos National Laboratory (2003).
3. Durham, J. S. *VARSKIN 3 A computer code for skin contamination dosimetry*. USNRC Report NUREG/CR-6918, Rev 0. U.S. Nuclear Regulatory Commission. (2006).
4. Attix, F. H. *Introduction to Radiological Physics and Radiation Dosimetry*. John Wiley & Sons (1986) ISBN 0471011460.
5. Shultis, J. K. and Faw, R. E. *Radiation Shielding*. American Nuclear Society (2000) ISBN 0894484567.
6. International Commission on Radiation Units and Measurements. *Tissue substitutes in radiation dosimetry and measurement*. ICRU Report 44 (1989).
7. Johns, H. E. and Cunningham, J. R. *The Physics of Radiology*. Charles C. Thomas (1983) ISBN 0398046697.